Xerogel synthesis from carbon materials and glue inspired by Japanese-solid-calligraphy ink

Sakurako Kubota, Fuwa Yoshioka, Masato Takada, Rui Itoh, Airi Uzawa, Arisa Ugawa, Kotone Masuda, Wakana Emizu, Junpei Hayakawa* [ID]

Science Team, Nara Prefectural Seiwaseiryo Senior High School, Shigigaoka 4-7-1, Sango, Nara 636-0813, Japan

*Corresponding author: Nara Prefectural Seiwaseiryo Senior High School, Shigigaoka 4-7-1, Sango, Nara 636-0813, Japan. Email: junpeih510@e-net.nara.jp

Abstract

Japanese-solid-calligraphy ink is a xerogel made by mixing soot and glue followed by molding and drying. Herein, we prepare xerogels from glue and 1 or 2 carbon materials (fullerene C_{60}, multiwalled and single-walled carbon nanotubes, nanodiamonds, graphite, graphene, and carbon nanohorns) and characterize their surface morphology, indentation hardness, surface resistivity, and other physical properties. Our ecofriendly and simple synthesis does not require special equipment and affords xerogels holding promise as electrode materials.

Keywords: carbon material, glue, xerogel.

Graphical Abstract
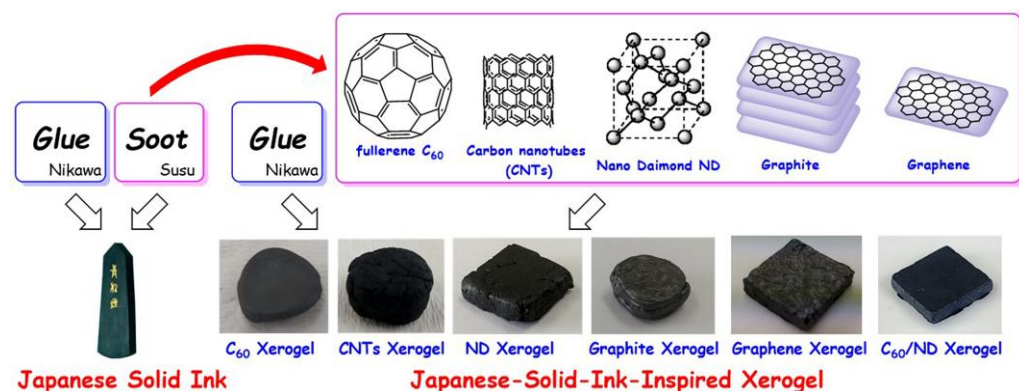
Japanese-solid-calligraphy ink, also known as *sumi*, has a long-standing history and is thought to have been introduced by Korea during the Tang dynasty.[1] Today, more than 1,000 yr later, the production of this ink remains a vital traditional industry in Japan. In particular, *sumi* is largely (95%) produced in the Nara Prefecture. Traditionally, Japanese-solid-calligraphy ink is made by mixing soot and glue, molding, and drying to produce esthetically appealing ingots suitable for preservation.

Soot contains fine carbon particles produced by the incomplete combustion of organic matter (e.g. pine or rapeseed oil),[2] while glue is primarily composed of gelatin extracted from the bones, skins, and tendons of animals (e.g. cattle, horses, rabbits, and fish).[3] During ink production, the fat-soluble carbon particles of soot are enclosed by the water-soluble particles of glue and therefore become dispersible in water. The resulting colloid dispersion (sol) is called liquid ink, "bokujū." Under appropriate conditions, the soot dispersion becomes gelatinous because of the sol-gel transformation of gelatin, and the resulting gel loses water upon drying to afford a xerogel, i.e. Japanese-solid-calligraphy ink.[4]

Previously, we focused on the colloid-protecting properties of glue and prepared novel glue-stabilized colloidal carbon dispersions that contain fullerene C_{60}, graphene, and multiwalled carbon nanotubes (MWCNTs) in place of soot.[5]

Carbon materials such as fullerene C_{60},[6] carbon nanotubes (CNTs),[7] nanodiamonds (NDs),[8] and graphene[9] have been actively studied owing to their remarkable structural and electrical properties. These materials hold promise for the production of pharmaceuticals and electronic materials. Additionally, carbon-containing composites have attracted considerable attention,[10] e.g. composites comprising fullerenes and lubricating oils reduce friction and improve wear resistance and have been put to practical use in engine oils.[11]
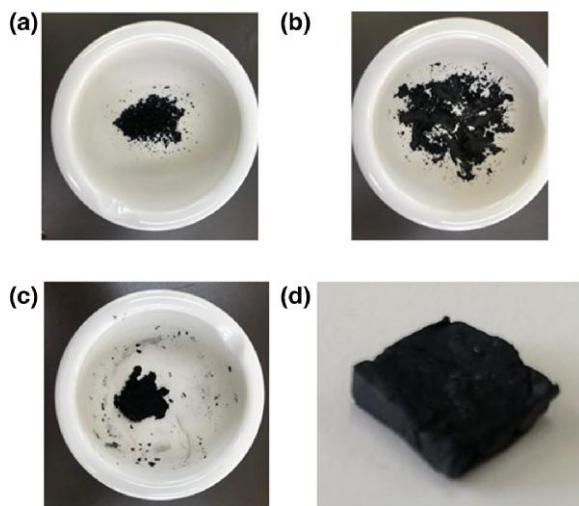
Fig. 1. Synthesis of xerogel with MWCNTs. Photographs of a) MWCNTs in a mortar, b) ground MWCNTs in a mortar, c) MWCNTs mixed with glue, and d) molded and dried MWCNT–glue mixture. The same technique was used for SWCNTs, fullerene C_{60}, graphite, graphene, NDs, and CNHs (Fig. 2).
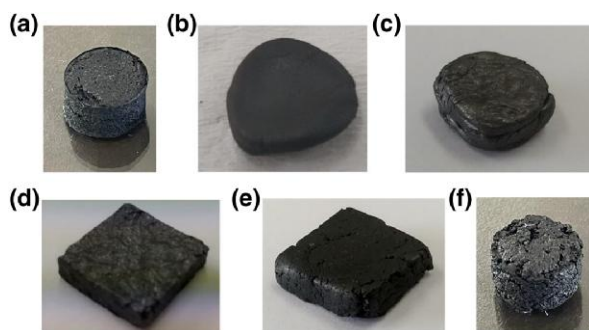

Fig. 2. Photographs of xerogels synthesized using a) SWCNTs, b) fullerene C_{60}, c) graphite, d) graphene, e) NDs, and f) CNHs.

Fig. 3. Photographs of xerogels synthesized using 2 types of carbon materials: a) MWCNTs/C_{60} (1:1, w/w), b) CNTs/graphene (1:1, w/w), c) MWCNTs/ND (1:1, w/w), d) C_{60}/graphene (1:1, w/w), and e) MWCNTs/C_{60} (1:4, w/w).

Fig. 4. Scanning electron microscopy images of a) MWCNTs (1,000×) and b) MWCNT xerogel (1,000×), c) SWCNTs (20,000×) and d) SWCNT xerogel (20,000×), and e) fullerene C_{60} (20,000×) and f) fullerene C_{60} xerogel (20,000×).

Actuators made from single-walled CNTs (SWCNTs) and ionic liquids are also of interest,[12] while NDs hold promise for drug delivery and the production of nontoxic ultraviolet light-shielding nanoadditives.[9] Considering the above, xerogels synthesized from glue and modern carbon materials should exhibit interesting physical properties. Sano et al.[13] used nitric acid to solubilize SWCNTs in water and dispersed them in gelatin to create a foam-like gel, while another study used gelatin and MWCNTs to create a hydrogel.[14] Herein, solid inks (xerogels) that contain dispersed carbon materials, such as fullerene C_{60}, CNTs, NDs, and graphite, were produced using traditional methods and characterized based on the findings of preparing carbon colloid solutions.[5]

Initially, we prepared a xerogel using MWCNTs as the carbon material, following a previously reported method for synthesizing soot-containing xerogels.[4] MWCNTs (500 mg) were placed in a mortar (Fig. 1a) and ground for 5 min (Fig. 1b). The powder was supplemented with 1 mL hot water containing 300 mg glue and ground for another 10 min (Fig. 1c). The resulting cake-like solid was shaped by pounding with a wooden mallet and dried to yield an MWCNT-containing xerogel (Fig. 1d, 384.1 mg). In this method, a technical loss of material containing glue and MWCNTs was observed during synthesis.
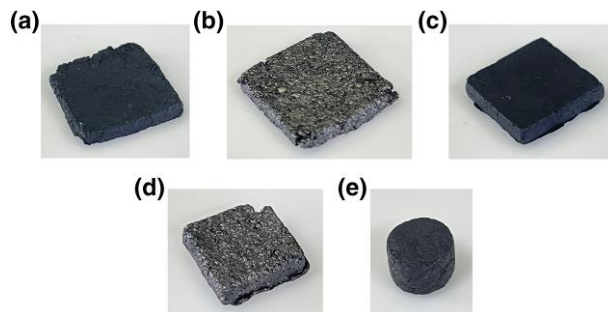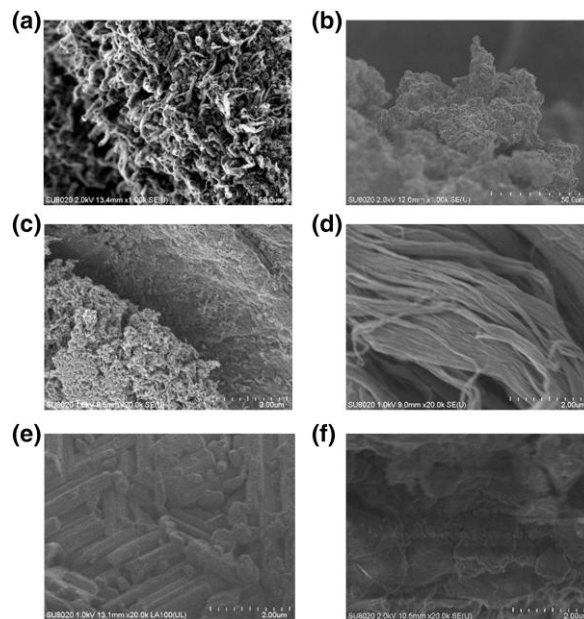
Furthermore, xerogels of arbitrary shapes can be synthesized using 2 types of carbon materials in various mass ratios (Fig. 3).

The physical properties of the synthesized xerogels were evaluated to examine their application potential. The surface morphology of the xerogels, observed by field-emission scanning electron microscopy (SU8020 TYPE II, Hitachi High-Technologies Corporation, Japan), significantly differed from that of the raw carbon materials. For example, the low-magnification (1,000×) imaging of MWCNTs showed that the raw material had a cocoon-like structure (Fig. 4a), whereas the MWCNT xerogel had a broccoli-like structure (Fig. 4b), which was indicative of efficient MWCNT dispersion. High-magnification (20,000×) imaging revealed that the orientation direction of raw SWCNTs (Fig. 4c) changed upon their incorporation into the corresponding xerogel (Fig. 4d), further demonstrating that the rod-like structure of raw C_{60} (Fig. 4e) was disintegrated in the corresponding xerogel (Fig. 4f).

Table 1. Physical properties of different xerogels.

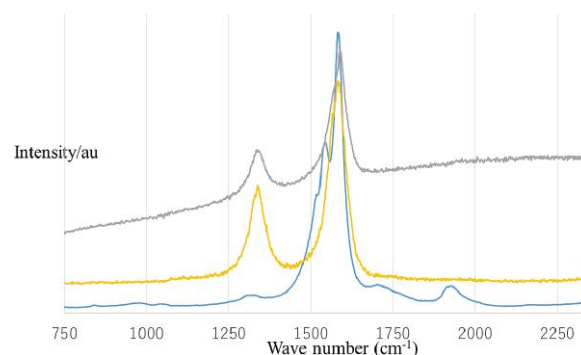| Entry	Xerogel	Density (g/cm^3)	Indentation hardness	Surface resistivity (Ω/cm^2)
1	Soot	1.02	95.6 ± 2.49	3.54×10^8
2	C$_{60}$	1.27	83.2 ± 2.22	6.55×10^{12}
3	NDs	1.07	78.9 ± 3.30	3.07×10^{11}
4	Graphite	1.27	86.1 ± 1.46	1.13×10^6
5	Graphene	1.03	74.2 ± 4.90	2.89×10^0
6	SWCNTs	1.20	93.3 ± 2.34	2.03×10^3
7	MWCNTs	1.15	76.1 ± 9.94	1.18×10^0
8	CNHs	1.21	99.7 ± 6.97	9.08×10^0
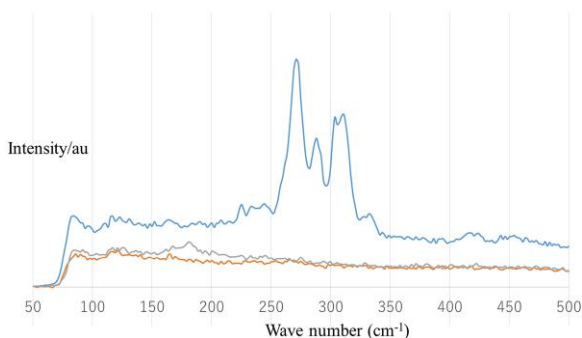
Fig. 5. Raman spectra of SWCNTs (blue), ground SWCNTs for 10 min in a mortar (orange), and the corresponding xerogel (gray) in the radial breathing mode region.

Fig. 6. Raman spectra of the raw SWCNTs (bottom line), ground SWCNTs for 10 min in a mortar (middle line), and corresponding xerogel (top line).

Table 2. Surface resistivities of xerogels containing 2 types of carbon materials.

Entry	Xerogel	Mass ratio	Surface resistivity (Ω/cm^2)
1	MWCNTs	…	1.18×10^0
2	C$_{60}$	…	6.55×10^{12}
3	MWCNTs/C$_{60}$	250:250	2.20×10^0
4	MWCNTs/C$_{60}$	100:400	1.71×10^1
5	MWCNTs/C$_{60}$	50:450	1.98×10^2
6	MWCNTs/C$_{60}$	25:475	3.74×10^4

The density of each xerogel was estimated from its volume and mass following thorough drying and was found to range from 1.0 to 1.3 g/cm^3 (Table 1).

Indentation hardness was measured using a durometer (Mitutoyo HH-332) and found to exhibit a considerable variation (Table 1).

Surface resistivity was measured using high-resistivity (Hiresta-UX MCP-HT800; Table 1, entries 1 to 4) and low-resistivity (Loresta AX MCP-T370; Table 1, entries 5 to 8) meters. C$_{60}$ and ND xerogels were found to be insulators (Table 1, entries 2 and 3), while soot and graphite xerogels (Table 1, entries 1 and 4) showed minimally lower resistivities, and graphene, SWCNT, MWCNT, and carbon nanohorn (CNH) xerogels showed resistivities in the semiconductor region (Table 1, entries 5 to 8). These results indicated that the xerogel surface resistivity strongly depended on the employed carbon material.

Figure 5 illustrates the Raman spectra of SWCNTs (Zeon) and the corresponding xerogel in the 100 to 300 cm^{-1} range, which corresponds to the radial breathing mode and provides insights into the SWCNT diameter. Although the employed raw SWCNTs primarily comprised tubes 3 to 5 nm in diameter, their spectrum showed a signal in the above region, suggesting the presence of SWCNTs with a diameter of 1 nm. The absence of such a signal in the xerogel spectrum indicates either a change in the SWCNT state or a decrease in the sample intensity of the xerogel at the time of detection. The Raman spectrum of the xerogel in the radial breathing mode region was similar to that of the ground raw material, SWCNTs, and the change in Raman spectrum could be expected to be due to mortar grating.

The high-frequency Raman spectra of the SWCNTs and corresponding xerogel (Fig. 6) featured D- and G-bands at 1,350 and 1,590 cm^{-1}, respectively. The D-to-G-band intensity ratio is known to be positively correlated with the defectiveness degree of CNTs. The spectrum of the raw material showed almost no D-band, indicating a low defectiveness degree, whereas a pronounced D-band was observed for the corresponding xerogel, suggesting that the SWCNT state had changed. The Raman spectrum of xerogel in this wavenumber range was also similar to that of the ground raw material, SWCNTs, and the change in the Raman spectrum can be expected to be due to the mortar grating.

The surface resistivities of the xerogels containing the 2 carbon materials (C$_{60}$ and MWCNTs) were measured. The surface resistivity of the xerogels containing MWCNTs was close to that of the MWCNT xerogel alone, which was 1.18×10^0 Ω/sq (Table 2, entries 3 to 6, entry 1). As the mass ratio of MWCNTs to C$_{60}$ decreased, the surface resistivity increased slightly, but it remained significantly lower compared to the resistivity of C$_{60}$, which was 6.55×10^{12} Ω/sq (Table 2, entry 2). For example, the surface resistivity of the sample with a MWCNT:C$_{60}$ mass ratio of 1:4 (100 mg MWCNTs + 400 mg C$_{60}$; Table 2, entry 4) was approximately 1 billionth of that of the xerogel containing C$_{60}$ only (Table 2, entry 2). The surface resistivities of xerogels containing both C$_{60}$ and MWCNTs are lower than those of C$_{60}$-only samples (Table 2). This result indicates that the MWCNTs were efficiently dispersed, i.e. did not aggregate in one part of the xerogel but formed a conductive network, as confirmed by scanning electron microscopy (Fig. 7).

To create conductive liquid ink (xerogel dispersion), a dispersion of CNH that most closely resembles the Japanese ink "bokujū" made from soot in appearance was prepared using the following procedure. The CNH xerogel (341.0 mg) was ground in a mortar and dispersed in water (3 mL).
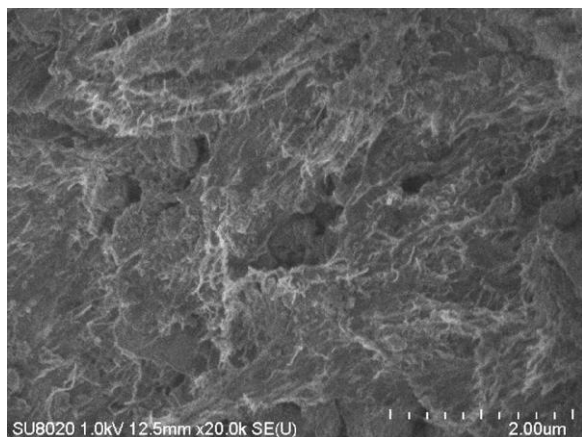
Fig. 7. Scanning electron microscopy image (20,000×) of an MWCNT/C_{60} xerogel (1:4, w/w).

The surface resistivity of the paper soaked in the resulting dispersion was 8.57×10^2 Ω/cm^2. Considering that the surface resistivities of the nonsoaked paper and paper soaked in the soot xerogel dispersion (*sumi* ink) were 3.62×10^{12} and 6.79×10^{10} Ω/cm^2, respectively, we concluded that the CNH xerogel can be used to fabricate conductive patterns on paper.

In summary, we synthesized xerogels that contain glue and various dispersed carbon materials, such as fullerene C_{60}, CNTs, NDs, graphite, graphene, and CNHs, and examined their physical properties and application potentials.

Acknowledgments

Supplementary data

Supplementary material is available at *Chemistry Letters* online.

Funding

Conflict of interest statement. None declared.

Data availability

The data that support the findings of this study are openly available.

References

1. S. Matsui, *The Japanese Ink (Japanese Title: THE SUMI)*, Higa Syuppansha, Tokyo, **1983**.
2. A. Ren, S. Kume, R. Baba, Y. Kishida, M. Fujiwara, S. Nakano, *Anal. Sci.* **2022**, *38*, 1149. https://doi.org/10.1007/s44211-022-00151-1
3. J. Alexander, *Glue and Gelatin, Classic Reprint*, American Chemical Society (Monograph Series), New York, **1923**.
4. F. Yoshioka, M. Takada, R. Itoh, A. Uzawa, J. Hayakawa, *J. Chem. Educ.* **2024**, *101*, 597. https://doi.org/10.1021/acs.jchemed.3c00933
5. K. Ishido, K. Nakamura, K. Taniyama, K. Fujita, K. Nakatani, Y. Nakagawa, J. Hayakawa, *J. Chem. Educ.* **2021**, *98*, 1381. https://doi.org/10.1021/acs.jchemed.0c00523
6a. A. Hirsch, *Angew. Chem. Int. Ed. Engl.* **1994**, *33*, 437. https://doi.org/10.1002/anie.199404371
6b. M. S. Dresselhaus, G. Dresselhaus, P. C. Eklund, *Science of Fullerenes and Carbon Nanotubes*, Academic Press, San Diego, **1996**.
7a. R. Saito, G. Dresselhaus, M. S. Dresselhaus, *Physical Properties of Carbon Nanotubes*, Imperial College Press, London, **1998**.
7b. S. Iijima, T. Ichihashi, *Nature* **1993**, *363*, 603. https://doi.org/10.1038/363603a0
8. V. N. Mochalin, O. Shenderova, D. Ho, Y. Gogotsi, *Nat. Nanotechnol.* **2012**, *7*, 11. https://doi.org/10.1038/nnano.2011.209
9. A. K. Geim, K. S. Novoselov, *Nat. Mater.* **2007**, *6*, 183. https://doi.org/10.1038/nmat1849
10. N. Agarwal, A. Rangamani, K. Bhavsar, S. S. Virnodkar, A. A. A. Fernandes, U. Chadha, D. Srivastava, A. E., Patterson, V. Rajasekharan, *Front. Mater.* **2024**, *11*, 1374034. https://doi.org/10.3389/fmats.2024.1374034
11. B. M. Ginzburg, L. A. Shibaev, O. F. Kireenko, A. A. Shepelevskii, M. V. Baidakova & A. A. Sitnikova, *Russ. J. Appl. Chem.* **2002**, *75*, 1330. https://doi.org/10.1023/A:1020929515246
12a. T. Fukushima, K. Asaka, A. Kosaka, T. Aida, *Angew. Chem. Int. Ed.* **2005**, *44*, 2410. https://doi.org/10.1002/anie.200462318
12b. R. H. Baughman, A. A. Zakhidov, W. A. de Heer, *Science (1979)* **2002**, *297*, 787. https://doi.org/10.1126/science.1060928
13. M. Nabeta, M. Sano, *Langmuir* **2005**, *21*, 1706. https://doi.org/10.1021/la047140x
14. A. O. Makarova, L. R. Bogdanova, O. S. Zueva, *Solid State Phenom.* **2020**, *299*, 299. https://doi.org/10.4028/www.scientific.net/ssp.299.299